THE JOURNAL OF BIOLOGICAL CHEMISTRY VOL. 284, NO. 24, pp. 16099–16107, June 12, 2009

Correlation of Vesicle Binding and Phospholipid Dynamics with Phospholipase C Activity

INSIGHTS INTO PHOSPHATIDYLCHOLINE ACTIVATION AND SURFACE DILUTION INHIBITION[*][S]

Received for publication, December 19, 2008, and in revised form, March 26, 2009 Published, JBC Papers in Press, March 31, 2009, DOI 10.1074/jbc.M809600200

Mingming Pu[‡], **Xiaomin Fang**[§], **Alfred G. Redfield**[§], **Anne Gershenson**[§], **and Mary F. Roberts**[‡1]

From [‡]*Boston College, Chestnut Hill, Massachusetts 02467 and* [§]*Brandeis University, Waltham, Massachusetts 02454*

The enzymatic activity of the peripheral membrane protein, phosphatidylinositol-specific phospholipase C (PI-PLC), is increased by nonsubstrate phospholipids with the extent of enhancement tuned by the membrane lipid composition. For *Bacillus thuringiensis* PI-PLC, a small amount of phosphatidylcholine (PC) activates the enzyme toward its substrate PI; above 0.5 mol fraction PC (X_{PC}), enzyme activity decreases substantially. To provide a molecular basis for this PC-dependent behavior, we used fluorescence correlation spectroscopy to explore enzyme binding to multicomponent lipid vesicles composed of PC and anionic phospholipids (that bind to the active site as substrate analogues) and high resolution field cycling ^{31}P NMR methods to estimate internal correlation times (τ_c) of phospholipid headgroup motions. PI-PLC binds poorly to pure anionic phospholipid vesicles, but 0.1 X_{PC} significantly enhances binding, increases PI-PLC activity, and slows nanosecond rotational/wobbling motions of both phospholipid headgroups, as indicated by increased τ_c. PI-PLC activity and phospholipid τ_c are constant between 0.1 and 0.5 X_{PC}. Above this PC content, PI-PLC has little additional effect on the substrate analogue but further slows the PC τ_c, a motional change that correlates with the onset of reduced enzyme activity. For PC-rich bilayers, these changes, together with the reduced order parameter and enhanced lateral diffusion of the substrate analogue in the presence of PI-PLC, imply that at high X_{PC}, kinetic inhibition of PI-PLC results from intravesicle sequestration of the enzyme from the bulk of the substrate. Both methodologies provide a detailed view of protein-lipid interactions and can be readily adapted for other peripheral membrane proteins.

Bacterial phosphatidylinositol-specific phospholipase C (PI-PLC)[2] enzymes aid in organism infectivity (1), whereas the structurally homologous mammalian PLCδ1 and related enzymes are required for phosphoinositide metabolism and are important for intracellular signaling (2, 3). These peripheral membrane proteins often have distinct binding modes for substrates and for other lipids that either anchor the protein to the surface or adjust its conformation to enhance catalysis (4). However, using traditional methods, it has been difficult to determine how lipid composition affects phospholipase binding and, conversely, how protein binding alters the lipid environment, particularly in multicomponent vesicles. Current methods for monitoring peripheral membrane protein binding to mixed component lipid vesicles, including centrifugation, gel filtration, and NMR, can provide information on bulk protein partitioning but do not usually provide insight into how the properties of the individual phospholipids change when protein is bound. Most of these methods also require protein concentrations well above the amounts used in enzyme kinetics. Therefore, even when binding to multicomponent vesicles can be measured, it has been difficult to separate how substrates (or substrate analogues) and activators interact with enzymes, such as PI-PLC, that catalyze interfacial reactions.

Protein binding to lipid vesicles or cells greatly retards protein translational diffusion. For fluorescently labeled proteins, this change can easily be monitored using fluorescence correlation spectroscopy (FCS) (5–7). FCS uses low protein concentrations (<1–50 nM), comparable with what is used in kinetic assays, and experiments can be performed in minutes. Thus, FCS allows us to screen different phospholipid compositions and to identify conditions that can be studied in detail by other techniques aimed at probing how protein binding alters the lipid environment. One such technique is high resolution field cycling ^{31}P NMR spectroscopy (fc-P-NMR) (8, 9).

Bacterial PI-PLCs recognize the headgroups of substrate, substrate analogue, and activator phospholipids, making ^{31}P NMR an obvious choice for studying protein-lipid interactions. Measurements of dipolar relaxation rates could, in principle, determine the effects of protein binding on headgroup orientation with respect to the bilayer normal as well as correlation times for different headgroup motions. However, in a typical modern spectrometer, the slow rotational diffusion time of lipid vesicles, the dominance of chemical shift anisotropy (CSA) relaxation, and a plethora of faster motions at higher fields pre-

* This work was supported, in whole or in part, by National Institutes of Health Grants GM60418 (to M. F. R.) and GM77974 (to A. G. R.).

[S] The on-line version of this article (available at http://www.jbc.org) contains supplemental Figs. S1 and S2.

[1] To whom correspondence should be addressed: Merkert Chemistry Center, Boston College, Chestnut Hill, MA 02467. Tel.: 617-552-3616; Fax: 617-552-2705; E-mail: mary.roberts@bc.edu.

[2] The abbreviations used are: PI-PLC, phosphatidylinositol-specific phospholipase C; PI, phosphatidylinositol; PLC, phospholipase C; AF488, Alexa Fluor 488 C_5; CSA, chemical shift anisotropy; DLS, dynamic light scattering; fc-P-NMR, high resolution field cycling ^{31}P NMR spectroscopy; FCS, fluorescence correlation spectroscopy; LUV, large unilamellar vesicles; PA, dioleoylphosphatidic acid; PC, 1-palmitoyl-2-oleoylphosphatidylcholine; PG, dioleoylphosphatidylglycerol; PMe, dioleoyl-phosphatidylmethanol; PS, dioleoylphosphatidylserine; SUV, small unilamellar vesicle; T, Tesla; GPI, glycosylphosphatidylinositol.

clude obtaining information on lipid structure and dynamics from relaxation rates. This limitation is avoided by fc-P-NMR spin lattice relaxation techniques that resolve the dynamics of each phospholipid component in mixed component vesicles by using the high field to separate resonances but allowing nuclei to relax at defined lower fields. To cycle the magnetic field, the sample is mechanically shuttled between the center high field region of the commercial NMR magnet's probe and a substantially lower magnetic field located above the probe before and after the delay times normally used in conventional NMR relaxation sequences (8). Analysis of the field dependence of spin lattice relaxation rates over a wide field range (0.002–11.7 T) provides several correlation times (τ) for each phospholipid molecule on time scales ranging from ps to μs and also allows us to separate dipolar and CSA interactions (8, 9). Of particular interest is the intermediate 5–10 ns τ_c that appears to be dominated by the wobbling of each phospholipid in the membrane (10). This τ_c provides a direct probe of lipid dynamics in these multicomponent membranes. A longer correlation time in the μs range, τ_v, provides information on how vesicle tumbling and lateral diffusion affect the phosphorus nuclei for each type of phospholipid in a mixed vesicle.

We have used FCS and fc-P-NMR to probe the interactions of *Bacillus thuringiensis* PI-PLC with small unilamellar vesicles (SUVs). This enzyme and related, secreted bacterial PI-PLCs are important for bacterial virulence, and explicit measurements of their interactions with lipids could aid in inhibitor design. Bacterial PI-PLCs are also structurally homologous to the catalytic domain of mammalian PLCδ1 and thus provide a good model for assessing how interactions of this domain with membrane components could modulate enzyme activity. *B. thuringiensis* PI-PLC has a solvent-accessible active site inserted into a relatively rigid ($\alpha\beta$)-barrel (11). The enzyme exhibits higher specific activity toward small unilamellar vesicles (~300 Å diameter) over larger vesicles with diameters of ≥1000 Å (12). For soluble substrates, the presence of phosphatidylcholine (PC) in micelles or vesicles activates the enzyme by decreasing the apparent K_m and increasing k_{cat} for both the phosphotransferase and phosphodiesterase steps (13). PC activation of PI cleavage, the interfacial reaction, also occurs with vesicle assay systems (12).

Our current model for kinetic activation of *B. thuringiensis* PI-PLC, based on the crystal structure of an interfacially impaired mutant protein (14) and extensive mutagenesis of surface residues (15–17), is that specific binding to PC in the lipid membrane allows key loop residues to penetrate the interface, promoting an enzyme conformation (suggested to be a transient dimer (14, 17)) with enhanced catalytic activity. However, in all PI vesicle assay systems examined, when the bulk PI is kept constant but the surface concentration decreases, PI-PLC specific activity decreases dramatically above $X_{PC} = 0.50$ (12, 18). This surface dilution inhibition is often interpreted as the result of the substrate surface concentration decreasing below a two-dimensional K_m measured in mole fraction PI (X_{PI}) units (19, 20). The affinity of the diluent (in this case PC) for the enzyme can also complicate a detailed interpretation of this kinetic effect. To truly understand this PI-PLC, where two discrete phospholipids are critical for optimal catalysis, we need a molecular level description of surface dilution inhibition.

Our results clearly indicate a role for lipid dynamics in PI-PLC activation by PC at low X_{PC} and reduced activity of PI-PLC at $X_{PC} > 0.5$. Specifically, these experiments reveal the following. (i) A relatively small amount of activator PC in the anionic lipid membrane promotes PI-PLC binding to vesicles. (ii) The affinity of the protein for vesicles increases as the amount of PC is increased. Affinities for SUVs reach a maximum for very PC-rich, but not pure PC, bilayers, indicating that *both* phospholipids contribute to tight vesicle binding (a synergistic effect between activator and active site binding of lipids). (iii) At moderate X_{PC}, $0.1 < X_{PC} < 0.5$, the dynamics of both phospholipids are affected similarly, and the restricted, slower motions, which are more or less independent of X_{PC}, parallel the high enzymatic activity. (iv) In the regime of tight binding to PC-rich bilayers, PC dynamics are preferentially slowed, suggesting that this activator lipid sequesters PI-PLC from the bulk of the substrate analogues, leading to significantly lower specific activity than would be expected. This latter observation provides a very specific interpretation of surface dilution inhibition as the result of tight binding of the protein to PC-rich regions that prevents its access to the bulk of the PI.

EXPERIMENTAL PROCEDURES

Vesicle Preparation and Sizing by Dynamic Light Scattering (DLS)—All lipid stock solutions (dioleoyl chains for all of the anionic phospholipids and 1-palmitoyl-2-oleoyl phosphatidylcholine as the PC species) in chloroform were purchased from Avanti Polar Lipids. The chloroform was removed under a stream of nitrogen gas, and the resultant film was lyophilized overnight. The lipid film was rehydrated with phosphate-buffered saline buffer, pH 7.3, for FCS experiments or 50 mM HEPES, pH 7.5, for enzyme assays and for ^{31}P NMR field cycling. Large unilamellar vesicles (LUVs) were prepared by multiple passages of the aqueous lipid solutions through polycarbonate membranes (100-nm pore diameter) using a miniextruder from Avanti. SUVs in phosphate-buffered saline, pH 7.3, were prepared by sonication (Branson Sonifier cell disrupter) of lipid mixtures for 30 min on ice. To introduce a fluorescent lipid into the SUVs, 1:20,000 mol fraction dipalmitoyl-lissamine-rhodamine phosphatidylethanolamine (Avanti) was added into the SUVs, and the mixture was sonicated for another 3 min. Under these conditions, a very small amount of fatty acid may be generated by hydrolysis of the phospholipids. However, no resonances for lyso-phospholipids were observed in a sample of PC/PI (1:1) treated in this fashion, indicating that the amount of lipid hydrolysis in this preparation was less than 0.5 mol %. Previous kinetic experiments have shown that small amounts of fatty acids do not affect enzyme specific activity (13).

The SUVs had a narrow vesicle size distribution as assessed by dynamic light scattering (21) using a Protein Solutions DynaProdynamic light scattering instrument from Wyatt Technology (22). The anion-rich SUVs were slightly smaller, with a narrower size distribution than PC-rich SUVs. All of the SUVs were used within 1 week of preparation.

PI-PLC—Recombinant *B. thuringiensis* PI-PLC was overexpressed in *E. coli* and purified as described previously (15). Protein concentrations were assessed by both 280 nm absorption and Lowry assays. Samples for fc-P-NMR were prepared with

10 mM total (dioleoylphosphatidylmethanol (PMe) plus PC) phospholipid and 0.5 or 3 mg/ml PI-PLC (0.014 or 0.086 mM) in 50 mM HEPES, pH 7.5. EDTA (1 mM) was present to scavenge any paramagnetic ions in solution. Fluorescently labeled PI-PLC was prepared from the N168C mutant protein, constructed using the QuikChange methodology (Stratagene). The altered gene sequence was confirmed by DNA sequencing (Genewiz). N168C was fluorescently labeled using Alexa Fluor 488 C_5 maleimide (AF488 maleimide; Invitrogen), according to the manufacturer's protocol. AF488 does not bind to vesicles (7), and this was confirmed by performing FCS experiments in the presence of free AF488 and SUVs. A labeling ratio of 100 ± 10% was determined by comparing the absorption of the protein at 280 nm with that of the probe at 495 nm.

PI-PLC Activity toward SUVs—Specific activities of recombinant *B. thuringiensis* PI-PLC toward PI in SUVs with varying mole fractions of PC were measured by ^{31}P NMR spectroscopy (13, 23). Each sample was in 50 mM HEPES, pH 7.5, with 1 mM EDTA and 0.1 mg/ml bovine serum albumin. In parallel to the fc-P-NMR studies, the total phospholipid concentration of the vesicles was 10 mM, with the mole fraction PC varying from 0.0 to 0.9. The amount of enzyme added, 0.2–5 μg (corresponding to concentrations of 5.8–144 nM), and the incubation time were chosen to allow less than 20% PI cleavage for each sample. Samples were incubated for fixed times at 28 °C, and the reaction was quenched by adding 40 μl of acetic acid to a 1-ml sample. Triton X-100 (100 μl) was added to solubilize the phospholipids for analysis by ^{31}P NMR. In these assays, myoinositol 1,2-(cyclic)-phosphate was the only product, and the specific activity was calculated according to integration of the myoinositol 1,2-(cyclic)-phosphate resonance compared with an internal standard (protons were not decoupled in these experiments).

FCS Measurements—FCS experiments were performed using a previously described (24) home-built confocal setup based on an IX-70 inverted microscope (Olympus). Further details on the apparatus and data treatment are provided in the supplemental material.

FCS experiments were carried out at 22 °C on 300-μl samples in phosphate-buffered saline, pH 7.3, plus 1 mg/ml bovine serum albumin, to stabilize PI-PLC, in chambered coverglass wells (LabTek). Prior to use, the chambers were coated with 10 mg/ml bovine serum albumin and rinsed with phosphate-buffered saline buffer to prevent protein adhesion to the sides of the wells. For PI-PLC vesicle binding experiments, 3.5 nM labeled protein was titrated with unlabeled vesicles. The substrate, PI, was not used for FCS experiments, because PI cleavage by PI-PLC produces diacylglycerol, leading to vesicle fusion (25). Thus, the anionic phospholipids PMe, PG, PA, or PS were used as substrate analogues. PG is a PI-PLC substrate and can be cleaved over a period of days by >1 mg/ml concentrations of PI-PLC (18, 26). However, at the low protein concentrations used in the FCS experiments, no detectable hydrolysis of PG occurred.

The auto- and cross-correlation, $G_{j,k}(\tau)$, were calculated from the time-dependent fluorescence intensities (27, 28). To measure the average diffusion coefficient of the SUVs, FCS experiments were performed on SUVs containing a small amount (0.5 μM) of rhodamine-labeled PC. Diffusion coefficients of free, AF488-labeled PI-PLC ($D_{\text{PI-PLC}}$) and labeled SUVs (D_{SUV}) were 58 ± 5 $\mu m^2\ s^{-1}$ (corresponding to a diffusion time (τ_D) = 173 μs) and 10.4 ± 1.0 $\mu m^2\ s^{-1}$ (τ_D = 1.48 ms), respectively.

In the presence of labeled PI-PLC and unlabeled lipid vesicles, FCS auto- and cross-correlations, $G(\tau)$, were analyzed using two-component, diffusion-only fits (5, 29),

$$G(\tau)=\frac{1}{\langle N\rangle}\left\{\begin{array}{l}(1-f)\left(\left(1+\dfrac{\tau}{\tau_{D,free}}\right)\sqrt{1+\dfrac{\tau}{S^2\tau_{D,free}}}\right)^{-1}\\ +\,f\left(\left(1+\dfrac{\tau}{\tau_{D,bound}}\right)\sqrt{1+\dfrac{\tau}{S^2\tau_{D,bound}}}\right)^{-1}\end{array}\right\} \quad \text{(Eq. 1)}$$

where $\langle N\rangle$ is the time-averaged number of PI-PLC molecules in the observation volume, f is the fraction of PI-PLC bound to vesicles, and $\tau_{D,\text{free}}$ and $\tau_{D,\text{bound}}$ are the diffusion times for free and vesicle-bound PI-PLC, respectively. For 488-nm excitation, values of S (related to the observation volume) were between 6.8 and 8.

High Resolution ^{31}P Field Cycling—The ^{31}P field cycling spin lattice relaxation rate (R_1) experiments were made at 25 °C on a Varian Unity$^{\text{plus}}$ 500 spectrometer using a standard 10-mm Varian probe in a custom-built device that moves the sample, sealed in a 10-mm tube, from the sample probe location to a higher position within, or just above, the magnet, where the magnetic field is between 0.06 and 11.7 T (8, 30). Spin lattice relaxation rates at each field strength were measured using 6–8 programmed delay times and analysis of the data with an exponential function to extract $R_1 = 1/T_1$. Although the details of the R_1 measurement for SUVs and the analysis to obtain and model R_1 as a function of field have been described previously (8, 9), a more detailed discussion of the methodology, data analysis, and associated assumptions is presented in the supplemental material.

The field dependence of the ^{31}P relaxation rates was analyzed in two discrete segments. R_1 from 0.06 up to 11.7 T was fit with contributions from three terms (8, 30): (i) dipolar relaxation associated with a correlation time, τ_c, typically in the 5–10 ns range and $R_c(0)$, the maximum relaxation rate for this correlation time, which is directly proportional to τ_c and inversely proportional to $r_{P\text{-}H}^{\ 6}$ ($R_c(0) = \tau_c\ (\mu_o/4\pi)^2\ (h/2\pi)^2\gamma_P^{\ 2}\gamma_H^{\ 2}\ r_{PH}^{\ -6}$), where $r_{P\text{-}H}$ indicates the average distance between the phosphorus and its nearest proton neighbors; (ii) CSA relaxation associated with the same slow correlation time (from which we can extract $S_C^{\ 2}$, an order parameter squared (8)); and (iii) CSA relaxation due to a faster motion (it is this term that dominates relaxation at high fields and is distinguished by a square law dependence). R_1 in the field range 0.06–11.7 T is then the sum of these three terms,

$$R_1 = (R_c(0)/2\tau_c)(0.1J(\omega_H - \omega_P) + 0.3J(\omega_P) + 0.6J(\omega_H + \omega_P)) + C_L\omega_P^2J(\omega_P) + C_HH^2 \quad \text{(Eq. 2)}$$

where $J(\omega) = 2\tau_c/(1 + \omega^2\tau_c^{\ 2})$, and the field, H, is the magnetic field measured in tesla; the coefficient $C_L = (1/15)(1 + \eta^2/3)\sigma^2S_C^{\ 2}$. In these expressions, γ represents the gyromag-

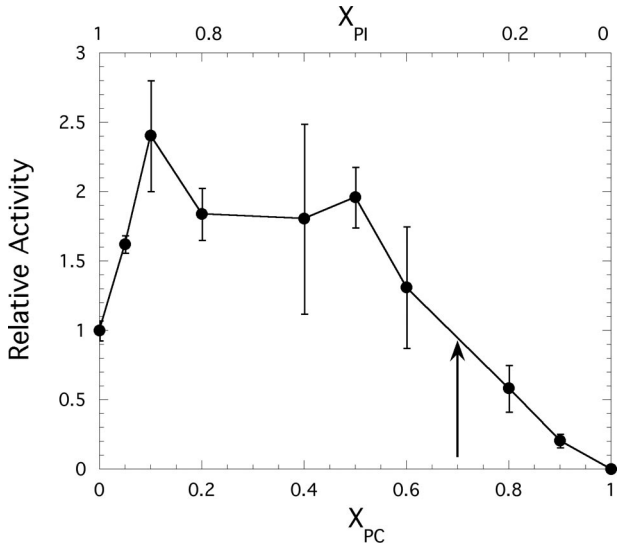

FIGURE 1. **Relative activity of *B. thuringiensis* PI-PLC toward SUVs with 10 mM total phospholipids as a function of the mole fraction of PC, X_{PC}.** The *arrow* indicates the X_{PC} value at which there is half-maximal enzyme activity as the amount of substrate is decreased.

netic ratio (for ^{1}H or ^{31}P), and σ and η are the CSA interaction size and asymmetry for phospholipids (8). The last term is for a faster motion and is not of interest in this work. A protein interacting with a given phospholipid would be expected to slow the motion associated with τ_c as well as increase S_C^2.

A second distinct increase in R_1 can be measured at very low fields (<0.03 T). The data in this low field regime are fit to a term added to $R_c(0)$ for dipolar relaxation with a submicrosecond correlation time, τ_v, and a maximum extrapolated relaxation rate of $R_v(0)$ for this slower motion (9).

$$R_1 = (R_v(0)/2\tau_v)(0.1J(\omega_H - \omega_P) + 0.3J(\omega_P) + 0.6J(\omega_H + \omega_P)) + R_c(0) \quad \text{(Eq. 3)}$$

The parameter τ_v primarily reflects vesicle tumbling, although lateral diffusion also contributes to this value. For two phospholipids in the same vesicle, a change in τ_v in the presence of protein can provide information on segregation of phospholipids (and faster lateral diffusion of one *versus* the other).

RESULTS AND DISCUSSION

PI-PLC Activity—The specific activity (μmol min^{-1} mg^{-1}) of PI-PLC toward PI-containing SUVs with a fixed enzyme and total lipid concentration (10 mM) and increasing mole fractions of the activator PC, X_{PC}, was determined. To emphasize the initial activation and eventual inhibition, the PI-PLC relative activity (specific activity normalized to the value obtained for pure PI SUVs, 91.3 ± 9.2 μmol min^{-1} mg^{-1}) is presented in Fig. 1. Although there is considerable error when averaging different series of experiments with SUVs, the trends are always the same. As little as 0.10 X_{PC} increases the enzyme activity toward PI 2–3-fold, and the activity is more or less constant from 0.10 to 0.50 X_{PC}. The magnitude of this activation depends on the concentration of PI and on the PC species; for example, a 7-fold activation was reported previously using 0.2 mol fraction dimyristoylphosphatidylcholine (12). Apparent K_m values for pure PI SUVs (derived from treating the system as if it followed Michaelis-Menten kinetics) have been estimated as 3–5 mM (12), which might suggest that the large kinetic effect of PC is from enhanced protein binding (12, 26).

Further increases in X_{PC} lead to a drop in PI-PLC-specific activity toward PI. In this case, the total phospholipid is kept constant, whereas the total and surface concentration of PI are decreased. Operationally, one can extract an interfacial "X_m" that represents the mole fraction of substrate in the interface needed for 50% of the maximum activity (analogous to a two-dimensional K_m for substrate). For *B. thuringiensis* PI-PLC, such an X_m is ~0.3 mol fraction PI ($X_{PI} = 1 - X_{PC}$). A wide variety of factors, including overall decreased vesicle binding, binding of nonsubstrate lipid in the active site, and/or altered lipid dynamics that make the substrate less accessible to bound protein, could decrease the specific activity as X_{PC} is raised while the total lipid concentration is fixed. To understand such kinetic effects, we need a separate analysis of bulk PI-PLC partitioning to vesicles with different compositions as well as insight into how the dynamics of each of the two lipids are affected when PI-PLC binds to the different interface compositions.

PI-PLC Binding to Binary Component SUVs—Changes in bulk binding of PI-PLC to SUVs can be assessed by FCS as long as a fluorescent probe attached to the protein does not alter the binding or enzyme activity. *B. thuringiensis* PI-PLC was labeled with AF488 maleimide at a single Cys residue introduced at Asn^{168} (N168C). Asn^{168} is on an exterior helix of *B. thuringiensis* PI-PLC, far from both the proposed protein dimerization interface (14) and the proposed lipid interface (11). N168C labeled with AF488 had a PI cleavage rate of 1600 ± 160 μmol min^{-1} mg^{-1} at 28 °C toward 8 mM PI dispersed in 32 mM diC$_7$PC micelles, the same value as for wild-type PI-PLC assayed under the same conditions.

Large unilamellar vesicles (typically ≥1000 Å in diameter) have generally been used for FCS studies of peptide or protein association with vesicles due to their higher thermodynamic stability and relatively uniform size (6, 7), although SUVs have occasionally been used (6, 29). The *B. thuringiensis* PI-PLC preferentially binds to small vesicles of PC (31), necessitating the use of SUVs for these binding experiments. SUVs composed of different ratios of PC to PMe or other anionic phospholipids, prepared by sonication, exhibited a narrow distribution of vesicle sizes as measured by DLS (Table 1). The average mass-weighted radius of the SUVs was 14.9 ± 2.7 nm, with 85 or more weight % of the lipids in vesicles with radii between 10 and 20 nm for all compositions.

For FCS binding experiments, 3.5 nM fluorescently labeled N168C PI-PLC was titrated with unlabeled SUVs. PI-PLC binding to SUVs shifted the correlation curves to longer times (Fig. 2*A*). The fraction of PI-PLC bound to the vesicles, *f*, was determined from two-component fits to the cross-correlations using the diffusion coefficients determined for Rho-labeled SUVs as well as for free PI-PLC. An example of how *f* varies with total phospholipid concentration at two fixed X_{PC} values is shown in Fig. 2*B*. A single PI-PLC binding site may be formed by multiple lipids, and the apparent dissociation constant K_d, representing the partitioning of the enzyme to the vesicle surface, as well as

TABLE 1

Dependence of PC/PMe SUV average radius on vesicle composition measured by dynamic light scattering

X_{PC}	r_{DLS}[a]	10 nm ≤ r ≤ 20 nm[b]
	nm	*weight %*
0.00	10.6 (10.0)[c]	98.5 (99.2)[c]
0.10	12.5	98.2
0.20	12.3	93.5
0.35	11.6	96.6
0.50	12.7	91.5
0.70	17.7	84.6
0.90	15.5	94.8
0.95	14.2	86.2
1.00	14.4	87.7

[a] The average radius for SUVs was calculated from the average diffusion coefficient D_{av} obtained from the light scattering experiment using the Stokes-Einstein relation.
[b] The weight percentage of the small vesicles whose radius fell between 10 and 20 nm as measured by DLS.
[c] The value in parentheses is for pure PG SUVs prepared by sonication.

the coefficient, n, used to account for a sigmoidal binding profile, were determined using Equation 4,

$$f = [PL]^n/(K_d^n + [PL]^n) \quad \text{(Eq. 4)}$$

where [PL] is the total phospholipid concentration, not the total vesicle concentration. For pure PC SUVs, the binding curve appears hyperbolic ($n = 1$).

The reported preference of *B. thuringiensis* PI-PLC for interacting with smaller, more curved vesicles (31) was confirmed by examining how the enzyme partitioned to PC LUVs (Fig. 2*C*). The K_d of PI-PLC binding to these LUVs was 60-fold higher than that for PC SUVs. The average radius for the population of LUVs to which the enzyme bound was determined using the Stokes-Einstein equation and the extracted D_{bound}. The calculated r_{FCS} was 25 ± 3 nm (corresponding to $D_{bound} = 8 \pm 1\ \mu m^2\ s^{-1}$), considerably smaller than the size of Rho-PE-labeled LUVs measured by FCS ($r_{LUV} = 40 \pm 9$ nm, corresponding to $D = 5 \pm 1\ \mu m^2\ s^{-1}$), or the mass-weighted average size of LUVs measured by light scattering ($r_{DLS} = 53 \pm 7$ nm), indicating that PI-PLC binds primarily to the smaller vesicles in the LUV population.

The composition of the vesicles (*i.e.* X_{PC}) as well as the identity of the anionic phospholipid affects PI-PLC binding to SUVs. The binding of the enzyme to SUVs as a function of X_{PC} was examined quantitatively using PMe, PG, PA, or PS as the anionic phospholipid. PG, PMe, and PA inhibit the enzyme competitively and serve as substrate analogues (32). Although PA can potentially have a charge of −2, its pK_{a2} is sufficiently high (8.3 for pure PA SUVs and 7.8 in vesicles with PC/PA = 4:1 (33)) that it is primarily a monoanion, as are the other anionic phospholipids examined. In these mixed vesicles, PS was the poorest PI-PLC binder, consistent with kinetic studies, where it is the weakest of the anionic phospholipid inhibitors (23, 32), and the protein has the highest affinity for mixed PC/PG SUVs (Fig. 3*A*). With the exception of PS, binding curves for all systems are sigmoidal for low X_{PC} vesicles (Fig. 3*B*). Although the average X_{PC} is known, individual SUVs can have X_{PC} values that are higher or lower than the average, and at low X_{PC}, PI-PLC may bind more tightly to the small subpopulation of vesicles with higher PC content (the number of vesicles in this subpopulation would of course increase as the total concentration of vesicles increased). Alternatively, several PC lipids may be needed to form the initial PI-PLC binding site, and the probability that PI-PLC will encounter such a transient PC-rich region increases in a cooperative fashion as the number of SUVs increases at low X_{PC}. Regardless of the detailed explanation for the sigmoidal appearance of the curves, it is obvious from our observations that a small amount of PC helps to anchor the enzyme to the mostly anionic phospholipid SUVs.

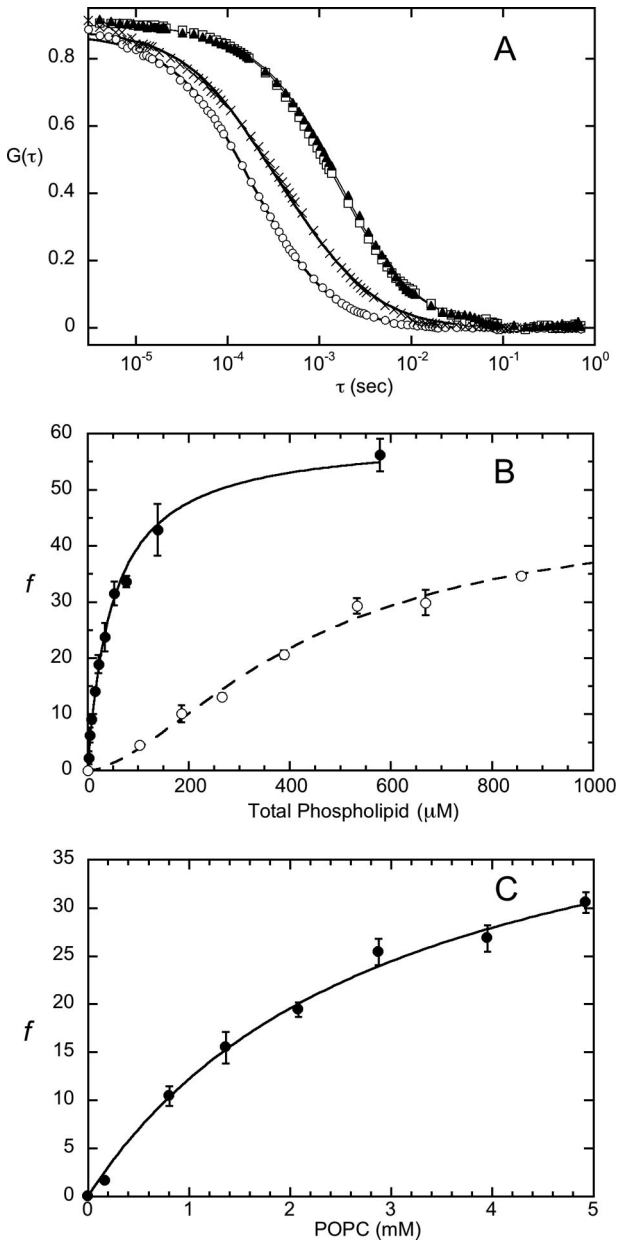

FIGURE 2. *A*, cross-correlation curves for free N168C-AF488-PI-PLC (○), Rho-labeled PC SUVs (□), and Rho-labeled PMe SUVs (▲). The *lines* through the data represent the best fit to Equation 1, with $f = 1$ (single species fit). The cross-correlation for 3.5 nM N168C-AF488-PI-PLC binding to 0.5 mM PC/PMe ($X_{PC} = 0.50$) SUVs (×), corresponding to 48% bound protein. The *line* through these data is the best fit to Equation 1. *B*, titration curves for N168C-AF488 PI-PLC binding to pure PC SUVs (●) and to 9:1 PMe/PC SUVs (○). The *lines* through the data represent the best fits to Equation 4. At high X_{PC}, the binding is not cooperative, although at low X_{PC}, the binding curves are clearly sigmoidal. *C*, fraction of labeled PI-PLC bound to PC LUVs as a function of PC concentration. The *line* is the best fit to Equation 4 ($n = 1$).

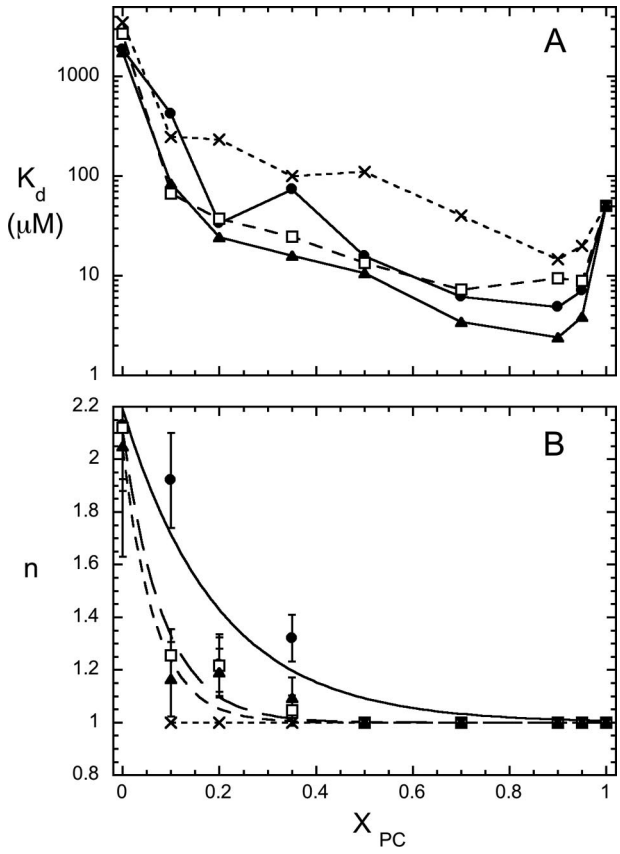

FIGURE 3. **Dependence of the PI-PLC binding to mixed anionic phospholipid/PC SUVs on X_{PC}.** Variation of K_d with X_{PC} (*A*) and variation of the cooperativity coefficient, *n*, with X_{PC} (*B*). The SUVs contained PC along with either PMe (●), PG (▲), PA (□) or PS (×).

For all of the anionic phospholipids mixed with PC, the apparent K_d has a bowl-shaped dependence on X_{PC} (Fig. 3*A*). There is a more than 10-fold drop in K_d for PG and PA at X_{PC} = 0.1, whereas PMe and PS show smaller, but still significant, decreases in K_d. The value of K_d continues to decrease and reaches a minimum at X_{PC} = 0.9 for all of the two-component vesicle systems. K_d then increases (typically 5–20-fold) for $X_{PC} > 0.90$. The observation of a minimum K_d as a function of X_{PC} demonstrates that both anionic phospholipid (substrate analogue) and PC help anchor the protein to these small vesicles. Clearly, the enzyme activity (Fig. 1) does not track bulk PI-PLC affinity for SUVs (Fig. 3*A*). Although activity reaches a plateau between 0.1 and 0.5 X_{PC} and then significantly decreases, the apparent K_d continues to decrease until X_{PC} = 0.9. Although one can think about bulk and two-dimensional binding constants to describe enzyme binding to phospholipids in vesicles, neither way of quantifying binding can explain the kinetic behavior on a molecular level.

Effects of PI-PLC Binding on Lipid Dynamics—Using fc-P-NMR, we demonstrated that PI-PLC binding affects the dynamics of the phospholipid in pure PC (but not pure PMe) SUVs (8). Here, we carry this observation further by studying the field dependence of the ^{31}P spin lattice relaxation rate, R_1, for PI-PLC binding to mixed PC/PMe SUVs. Examples of R_1 field dependence profiles for each phospholipid in the very low field region (0–0.05 T) and higher field region (0.07–11.74 T) are shown in Fig. 4 for two different X_{PC} values. In the presence of PI-PLC, the field dependence above 0.07 T for PC (Fig. 4*B*) and PMe (Fig. 4*D*) are similar at X_{PC} = 0.2 but noticeably different at X_{PC} = 0.8, where $R_c(0)$ is clearly larger for the PC component. The relaxation profile in the absence of PI-PLC is shown as a *gray line* in each *panel* in Fig. 4. Without protein, τ_c for the two phospholipids is the same, 5.6 ± 0.5 ns, and does not vary significantly with X_{PC}. Quantifying the changes induced by protein provides insight into how PI-PLC binding affects the dynamics of *each* phospholipid.

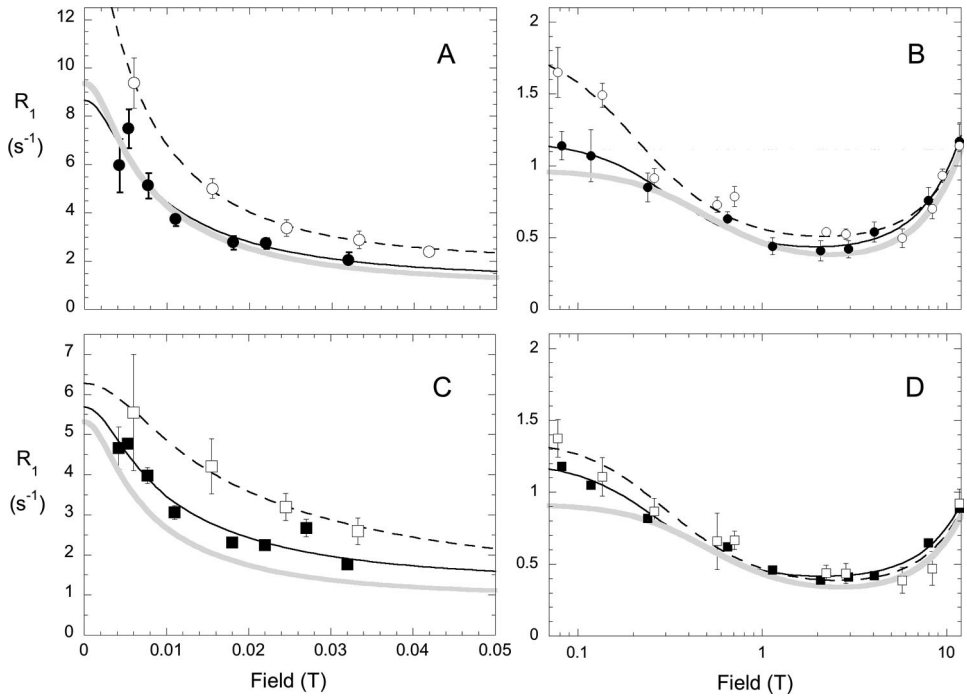

FIGURE 4. **Field dependence of R_1 for PC and PMe in mixed SUVs with X_{PC} = 0.20 (*filled symbols*) or X_{PC} = 0.80 (*open symbols*) and 3 mg/ml (86 μM) PI-PLC.** *A*, field dependence of the PC R_1 from 0 to 0.05 T. *B*, PC R_1 from 0.07 to 11.7 T. The field dependence of the PMe R_1 is shown from 0 to 0.05 T (*C*) and from 0.07 to 11.7 T (*D*). The curves through these points represent the best fits to the simple model for R_1 dependence on field with two correlation times (τ_v from *A* and *C* and τ_c from *B* and *D*). The profile exhibited by the phospholipid in the absence of protein is shown in each *panel* by the *gray line*.

The rise in relaxation rate, R_1, below 1 T is caused by dipolar relaxation, principally through dipolar interactions with the glycerol C(3) protons (8). As the field is increased above 1 T, relaxation due to CSA becomes important. As described in detail in the supplemental material, a model-free approach was used to fit the field-dependent profile for R_1 from 0.07 up to 11.7 T as a sum of dipolar and CSA terms associated with a slow, τ_c (ns), and fast, τ_h (ps), motion and to estimate $R_c(0)$, the maximum relaxation rate caused by τ_c-associated motions. This τ_c has been modeled by diffusive and wobbling motions of each phospholipid

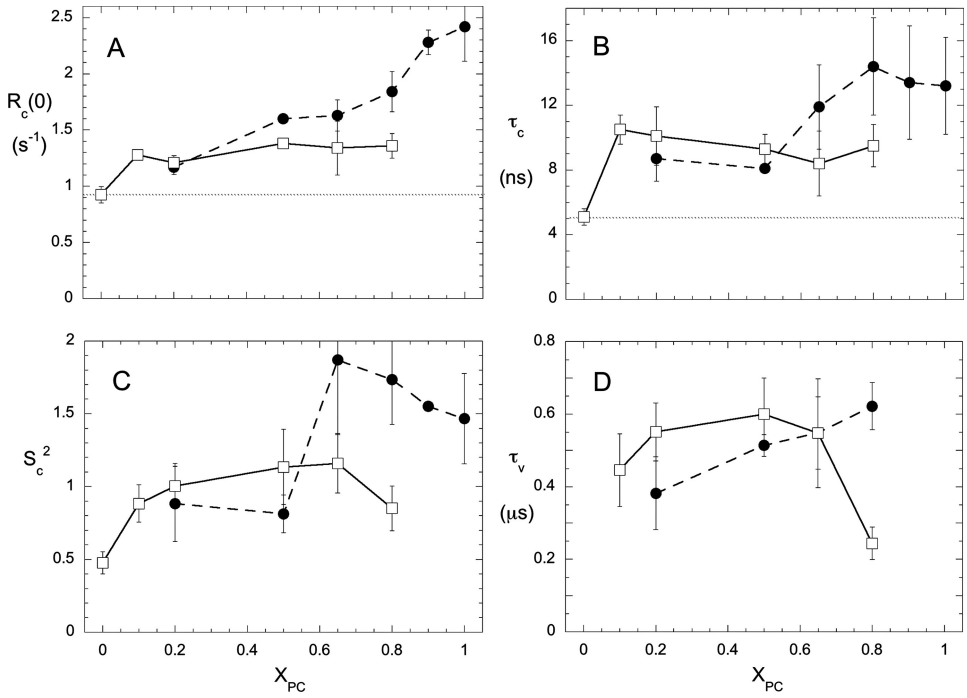

FIGURE 5. **Variation of parameters extracted from high resolution ^{31}P field cycling for PC (●) and PMe (□) in mixed vesicles as a function of X_{PC}.** *A*, $R_c(0)$; *B*, τ_c; *C*, S_C^2; *D*, τ_v. The concentration of PI-PLC was 3 mg/ml (86 μM) for all X_{PC} except 0.65 and 0.90, for which 0.5 mg/ml (14 μM) PI-PLC was present. The *dotted lines* in *A* and *B* show the values for PMe in the absence of protein.

treated as a relatively rigid cylinder encompassing the phosphorus-glycerol-acyl chains in a hexadecane-like medium (10).

The addition of PI-PLC to pure PMe SUVs had very little effect on τ_c and $R_c(0)$ (8) under conditions (10 mM PMe) where the FCS K_d (3 ± 1 mM) indicates that most of the protein is associated with the SUVs. Therefore, the average PMe molecular environment is not significantly perturbed, and interactions between the SUVs and PI-PLC are probably electrostatic and nonspecific. In contrast, when PI-PLC was added to pure PC vesicles, it significantly increased τ_c (from 5 to ~13 ns) as well as increasing $R_c(0)$ 2–3-fold. The tight binding of PI-PLC to PC SUVs, as measured by FCS (Fig. 3*A*), clearly involves significant retardation of PC motion in the ns range. An order parameter, S_c^2, extrapolated from the CSA portion of relaxation (8), is ~0.5 for both phospholipids in the absence of enzyme. For PC SUVs with PI-PLC bound, this parameter has a value greater than 1 (8). Given uncertainties in several of the input parameters used to determine S_c^2 (*e.g.* CSA interaction size and asymmetry), the absolute value of this order parameter may not be correct. However, for these two-component SUVs, changes in S_c^2 serve as a convenient way to compare the effects of PI-PLC binding on lipid motions as a function of X_{PC}.

For X_{PC} between 0 (pure PMe) and 1 (pure PC), both phospholipids show changes in the field dependence of R_1 only when the PI-PLC is present. In these experiments, as in the activity assays, the total concentration of phospholipids was fixed at 10 mM, but the PI-PLC concentration was considerably higher (86 μM), resulting in a lipid/PI-PLC ratio of 116:1. Centrifugation of samples through an Amicon Centricon-100 filter showed that about 20–40% of the protein was associated with the SUVs under these conditions. This suggests that there is adequate enzyme to saturate all vesicle binding sites. Two X_{PC} points, 0.1 and 0.65, used a lipid/PI-PLC ratio of ~700:1 with only minor effects on τ_c and $R_c(0)$ compared with the higher protein concentration. All protein was bound to the vesicle at the end of the experiment, consistent with saturation of the vesicles with a total phospholipid/PI-PLC of ~400–500.

For each X_{PC}, analysis of the field dependence of R_1 from 0.06 to 11.7 T in the presence of PI-PLC was used to extract $R_c(0)$ and τ_c for each of the two phospholipids in the SUVs. As shown in Fig. 5, as little as 0.1 X_{PC} increased $R_c(0)$ and τ_c for PMe significantly, and both parameters were roughly constant from 0.1 to 0.5 X_{PC} and similar to the values for PC in the same vesicle. The presence of PC in these mostly anionic phospholipid SUVs allows PI-PLC to bind, and as a consequence, the ns motion of both phospholipids is hindered, and τ_c increases from 5 ns. (This is easily seen in Fig. 4, *B* and *D*, where R_1 at ~0.1 T is significantly higher in the presence of PI-PLC than it is in the absence of protein (*gray line*).) These effects of PI-PLC are also reflected in the S_C^2 values for PMe, which increase as soon as PC is added (Fig. 5*C*). The PC resonance in the SUVs is broader than for PMe, so the field dependence of R_1 for PC at $X_{PC} = 0.10$ could not be obtained with any accuracy. Nonetheless, the fc-P-NMR data reveal that for X_{PC} values of 0.5 or less, the phosphorus motions of both PMe and PC are similarly restricted with PI-PLC present. These effects of the protein on phospholipid dynamics could reflect chemical exchange between active site or activator site and bulk phospholipid or else a generalized change in membrane fluidity/viscosity as long as the protein is transiently anchored to the bilayer.

At $X_{PC} > 0.5$, there is a switch in phospholipid behavior with PI-PLC, resulting in a significantly increased $R_c(0)$, τ_c, and S_c^2 for PC but not for PMe in the same SUV (Fig. 5). For PC, the extracted value of S_c^2 is greater than 1, a likely reflection of our not quite correct assumption that τ_c is the same for CSA and dipolar terms (for a discussion of this, see the supplemental material). However, what is important is that S_c^2 increases for PC but not for PMe as this lipid becomes the major component in these vesicles. Clearly, PI-PLC differentially hinders the PC motions at $X_{PC} > 0.5$. The difference in parameters for the two phospholipids suggests that chemical exchange (between protein-bound and "free" in the bilayer) rather than bulk membrane fluidity is the major determinant of τ_c for each phospholipid.

So what does PI-PLC actually do to PC in high X_{PC} bilayers? One interpretation is that PC can now interact with the enzyme active site. The motion of the larger (compared with PMe) PC

headgroup might be more restricted at this second binding site. However, the FCS results indicate that even at high X_{PC}, PMe and PC behave synergistically when binding to PI-PLC. It has also been shown that PI-PLC bound to pure PC SUVs is activated toward the soluble substrate myoinositol 1,2-(cyclic)-phosphate (13). Thus, the active site is unlikely to be occupied by PC acting as a competitive inhibitor. A different explanation for the observed fc-P-NMR effects is that there is a preferential interaction of PI-PLC with PC, resulting in lipid clustering.

The field dependence of the relaxation rate at very low (<0.06-T) fields provides hints that PI-PLC-induced partial separation of PC and PMe may occur at $X_{PC} > 0.5$. From the low field rise in relaxation rate (Fig. 4, *A* for PC and *C* for PMe), we can determine a correlation time, τ_v, for each phospholipid, which in the absence of protein is related to the vesicle size and includes contributions from vesicle tumbling, lateral diffusion, and possibly other slower (100-ns) motions of the phospholipids (9). For these sonicated vesicles, the average diameter, as measured by DLS, is relatively constant as X_{PC} is increased from 0 to 0.8 (Table 1). At low X_{PC}, τ_v is similar for both phospholipids (0.4–0.5 μs). This value is 2–3 times shorter than would be expected for overall rotation of SUVs (9), consistent with some contribution from lateral diffusion. However, as X_{PC} increases above 0.5, τ_v for PC increases slightly (from 0.51 ± 0.03 μs at $X_{PC} = 0.5$ to 0.62 ± 0.06 μs at $X_{PC} = 0.8$), whereas the value for PMe decreases to 0.25 ± 0.07 μs at the highest X_{PC} where relaxation in the low field region was examined (Fig. 5*D*). That τ_v for PMe is reduced can be seen in Fig. 4*C*, where the curves for both X_{PC} values have similar $R_v(0)$ values but the midpoint for this change occurs at a higher field for $X_{PC} = 0.8$, the hallmark of a shorter correlation time. For comparison, the analysis of the low field dependence of pure PMe SUVs (see Fig. S2) yields a τ_v of 0.39 ± 0.03 μs. In the PC-rich SUVs with PI-PLC added, τ_v for PMe is considerably less than that for PC, and the decrease in τ_v for PMe as X_{PC} increases is statistically significant. The decrease in τ_v for bulk PMe indicates that the PMe lateral diffusion, unfettered by protein (and perhaps neighboring PC molecules), is now more effective at relaxing the residual magnetization of ^{31}P. This would occur if PC molecules sequester the protein from PMe, which now has a shorter path around the vesicle in areas devoid of PC/protein clusters.

PC Activation and Inhibition of PI-PLC, a Phospholipid-centric View—The combination of FCS and fc-P-NMR provides new insights into the role of PC in *B. thuringiensis* PI-PLC-catalyzed PI cleavage. In moderate ionic strength buffers, PI-PLC has very weak affinity for SUVs containing only anionic lipids, in this case the substrate PI (or analogue, such as PMe), and relatively small amounts of PC serve to anchor the protein to the mixed component bilayers. The hallmark of that binding is that the rotational/wobbling motion of both substrate analogue (PMe) and activator (PC) molecules is similarly reduced for each phospholipid. However, tight binding does not necessarily correlate with higher enzyme activity. As the relative amount of PC, X_{PC}, is increased above 0.5, specific activity decreases, and there is a change in the dynamics of PC bound to PI-PLC; in contrast, the affinity of the protein for SUVs (as measured by the apparent K_d) continues to increase up to 0.90 X_{PC}.

In kinetic models for surface active enzymes (19, 20), a decrease in activity with increasing mole fraction of diluent is often attributed to the reduction of the substrate surface concentration below a threshold two-dimensional K_m. Our data reveal that decreased *B. thuringiensis* PI-PLC activity at high PC is correlated with changes in substrate (PI) and diluent (PC) lipid-protein interactions and lipid dynamics. Assuming that PMe is a reasonable stand-in for the substrate, at high X_{PC}, PC dynamics, reflected in τ_v, τ_c, and S_c^2 for the PMe/PC system, would be much slower than PI dynamics in the same vesicle. PI may still be bound at the active site even at high X_{PC}, as reflected by the continued synergy between the two types of phospholipids in vesicle binding, but it would not be rapidly exchanging with the bulk PI pool. By analogy to the PMe/PC system, the tightly bound enzyme is clustered with PC and sequestered from much of the PI substrate in the bilayer. This sequestration probably inhibits PI-PLC diffusion around a given vesicle as well as release from one vesicle and binding to another for cleavage of more PI. We propose that the changes in protein-lipid interactions detected by fc-P-NMR generate the observed decrease in PI-PLC activity at high X_{PC}, either in the kinetic experiment shown here, where total phospholipid is a constant and X_{PC} is varied, or in the more usual surface dilution experiments, where PI is constant and X_{PC} increases. Such behavior, differential interactions of an enzyme with substrate and diluent amphiphiles that affect substrate accessibility to enzyme as well as lipid dynamics in the bilayer, may also be responsible for the decreased activity seen in the high diluent regime for many other phospholipases. The combination of FCS and fc-P-NMR encompassing bulk binding and phospholipid dynamics can be easily generalized to other, less well studied phospholipases or other peripheral membrane proteins where specific phospholipids are thought to have differential binding effects on enzymes.

Biological Relevance of PI-PLC/PC Interactions—The effects of PI-PLC on this simple two-component bilayer provide insights into the biological role of this enzyme secreted by different *Bacillus* strains. *B. thuringiensis* is an insect pathogen, and earlier work showed that an avirulent mutant lacking both the broad range and PI-specific PLC was much less potent in killing cells (34). In this insect model, wild type *B. thuringiensis* disappeared from the circulation hours after injection, while the mutant organism was still circulating. This suggested that one or both phospholipases contributed to the early stages of infection and association of the bacteria with insect and mammal cells, since *B. thuringiensis* is also an opportunistic human pathogen leading to pulmonary infections (35). Membrane-damaging factors, such as the PI-PLC, apparently allow the bacteria to persist in that environment.

More recent work with *Bacillus anthracis* has also provided evidence that *B. anthracis* PI-PLC, a secreted PI-PLC with high sequence similarity to *B. thuringiensis* PI-PLC, contributes to bacterial pathogenicity. The *B. anthracis* PI-PLC, like the enzyme from *B. thuringiensis*, can cleave GPI-anchored proteins in plasma membranes as well as intracellular PI, providing two potential roles for this enzyme in virulence. *B. anthracis* PI-PLC has also been shown to down-modulate the immune

response, and this appears to involve its ability to cleave GPI-anchored proteins (1).

Access to GPI anchors on the external leaflet of a target cell would be facilitated by protein binding to PC (or sphingomyelin, also an activator). GPI anchors may exist in clustered domains (36), indicating that PI-PLC cleavage of GPI anchors may occur at low X_{PC}.

In *B. anthracis*, PI-PLC is one of three phospholipase C enzymes that contribute to macrophage-associated growth of the bacteria (37). Along with aiding bacterial association with the macrophages, the three enzymes may have overlapping roles in pathogenesis by aiding in release from the phagocyte (38). Since the interior leaflet of the phagocyte resembles the external leaflet of the plasma membrane, PC will be present for PI-PLC binding. Even if PI and GPI-anchored targets are not available, the strong interaction of this PI-PLC with PC in the membrane could cause clustering of the PC, making the phagocyte more susceptible to other membrane hydrolytic factors.

Acknowledgments—We thank Professor Irving Epstein for use of the DynaProdynamic light scattering instrument and Dr. Vladimir Vanag for assistance with the light scattering experiments.

REFERENCES

1. Zenewicz, L. A., Wei, Z., Goldfine, H., and Shen, H. (2005) *J. Immunol.* **174,** 8011–8016
2. Downes, C. P., Gray, A., and Lucocq, J. M. (2005) *Trends Cell Biol.* **15,** 259–268
3. Rhee, S. G. (2001) *Annu. Rev. Biochem.* **70,** 281–312
4. Mulgrew-Nesbitt, A., Diraviyam, K., Wang, J., Singh, S., Murray, P., Li, Z., Rogers, L., Mirkovic, N., and Murray, D. (2006) *Biochim. Biophys. Acta* **1761,** 812–826
5. Magde, D., Elson, E. L., and Webb, W. W. (1974) *Biopolymers* **13,** 29–61
6. Rhoades, E., Ramlall, T. F., Webb, W. W., and Eliezer, D. (2006) *Biophys. J.* **90,** 4692–4700
7. Rusu, L., Gambhir, A., McLaughlin, S., and Rädler, J. (2004) *Biophys. J.* **87,** 1044–1053
8. Roberts, M. F., and Redfield, A. G. (2004) *J. Am. Chem. Soc.* **126,** 13765–13777
9. Roberts, M. F., and Redfield, A. G. (2004) *Proc. Natl. Acad. Sci. U. S. A.* **101,** 17066–17071
10. Klauda, J. B., Roberts, M. F., Redfield, A. G., Brooks, B. R., and Pastor, R. W. (2008) *Biophys. J.* **94,** 3074–3083
11. Heinz, D. W., Ryan, M., Bullock, T. L., and Griffith, O. H. (1995) *EMBO J.* **14,** 3855–3863
12. Qian, X., Zhou, C., and Roberts, M. F. (1998) *Biochemistry* **37,** 6513–6522
13. Zhou, C., Wu, Y., and Roberts, M. F. (1997) *Biochemistry* **36,** 347–355
14. Shao, C., Shi, X., Wehbi, H., Zambonelli, C., Head, J. F., Seaton, B. A., and Roberts, M. F. (2007) *J. Biol. Chem.* **282,** 9228–9235
15. Feng, J., Wehbi, H., and Roberts, M. F. (2002) *J. Biol. Chem.* **277,** 19867–19875
16. Feng, J., Bradley, W. D., and Roberts, M. F. (2003) *J. Biol. Chem.* **278,** 24651–24657
17. Guo, S., Zhang, X., Seaton, B. A., and Roberts, M. F. (2008) *Biochemistry* **47,** 4201–4210
18. Volwerk, J. J., Filthuth, E., Griffith, O. H., and Jain, M. K. (1994) *Biochemistry* **33,** 3464–3474
19. Carman, G. M., Deems, R. A., and Dennis, E. A. (1995) *J. Biol. Chem.* **270,** 18711–18714
20. Berg, O. G., Gelb, M. H., Tsai, M. D., and Jain, M. K. (2001) *Chem. Rev.* **101,** 2613–2654
21. Maulucci, G., De Spirito, M., Arcovito, G., Boffi, F., Castellano, A. C., and Briganti, G. (2005) *Biophys. J.* **88,** 3545–3550
22. Schuck, P. (2000) *Biophys. J.* **78,** 1606–1619
23. Volwerk, J. J., Shashidhar, M. S., Kuppe, A., and Griffith, O. H. (1990) *Biochemistry* **29,** 8056–8062
24. Liu, L., Mushero, N., Hedstrom, L., and Gershenson, A. (2006) *Biochemistry* **45,** 10865–10872
25. Goñi, F. M., and Alonso, A. (2000) *Biosci. Rep.* **20,** 443–463
26. Zhou, C., Qian, X., and Roberts, M. F. (1997) *Biochemistry* **36,** 10089–10097
27. Elson, E. L., and Magde, D. (1974) *Biopolymers* **13,** 1–27
28. Thompson, N. L. (1991) in *Topics in Fluorescence Microscopy* (Lakowicz, J., ed) pp. 337–378, Plenum Press, New York
29. Takakuwa, Y., Pack, C. G., An, X. L., Manno, S., Ito, E., and Kinjo, M. (1999) *Biophys. Chem.* **82,** 149–155
30. Roberts, M. F., Cui, Q., Turner, C. J., Case, D. A., and Redfield, A. G. (2004) *Biochemistry* **43,** 3637–3650
31. Wehbi, H., Feng, J., Kolbeck, J., Ananthanarayanan, B., Cho, W., and Roberts, M. F. (2003) *Biochemistry* **42,** 9374–9382
32. Zhou, C., and Roberts, M. F. (1998) *Biochemistry* **37,** 16430–16439
33. Swairjo, M. A., Seaton, B. A., and Roberts, M. F. (1994) *Biochim. Biophys. Acta* **1191,** 354–361
34. Zhang, M. Y., Lövgren, A., Low, M. G., and Landén, R. (1993) *Infect. Immun.* **61,** 4947–4954
35. Ghelardi, E., Celandroni, F., Salvetti, S., Fiscarelli, E., and Senesi, S. (2007) *Microbes Infect.* **9,** 591–598
36. Paulick, M. G., and Bertozzi, C. R. (2008) *Biochemistry* **47,** 6991–7000
37. Heffernan, B. J., Thomason, B., Herring-Palmer, A., Shaughnessy, L., McDonald, R., Fisher, N., Huffnagle, G. B., and Hanna, P. (2006) *Infect. Immun.* **74,** 3756–3764
38. Heffernan, B. J., Thomason, B., Herring-Palmer, A., and Hanna, P. (2007) *FEMS Microbiol. Lett.* **271,** 98–105